$B \to K^* l^+ l^-$ a portal for New Physics? A new insight on the Anomaly

Joaquim Matias
Universitat Autònoma de Barcelona

LaThuile

Based on: S. Descotes, J. M., J. Virto, **Phys. Rev. D88 (2013) 074002**

J. M. and N. Serra, **arXiv:1402xxxx**

February 27, 2014

PLAN of the TALK

PART I Status of the Theoretical Analysis of LHCb data using the clean observables P_i'.
Understanding of the observed anomaly using an effective Hamiltonian approach.
First **update** including experimental correlations.

PART II A fully new insight on the anomaly based on **symmetries**:
A new relation between P_2, the zero of A_{FB} and the anomaly in P_5'.

PART III An explanation of the small controversy on C_9'.

Conclusions

The lack of any evidence for NP in direct searches after the discovery of a SM-like Higgs, leave us at present and in the short term as the best paradigm to unveil **New Physics** *(at least in Flavour)*:

$$\mathcal{L} = \sum_i (C_i^{SM} + \mathbf{C_i^{NP}})\mathcal{O}_i + \sum_j \mathbf{C'_j}\mathcal{O}'_j$$

an accurate (over constraining) determination of Wilson coefficients:

a) to observe deviations $\mathbf{C_i^{NP}}$ or **b)** emergence of new operators ($\mathcal{O}'_j$ or scalars).

In particular those associated to operators (and chiral counterparts $\mathcal{O}'_{7,9,10}$ (L $\leftrightarrow$ R):

$$\mathcal{O}_\mathbf{7} = \frac{e}{16\pi^2} m_b(\bar{s}\sigma_{\mu\nu}P_R b)F^{\mu\nu}, \quad \mathcal{O}_\mathbf{9} = \frac{e^2}{16\pi^2}(\bar{s}\gamma_\mu P_L b)(\bar{\ell}\gamma^\mu \ell), \quad \mathcal{O}_\mathbf{10} = \frac{e^2}{16\pi^2}(\bar{s}\gamma_\mu P_L b)(\bar{\ell}\gamma^\mu \gamma_5 \ell),$$

Wilson coefficients $[\mu_b = \mathcal{O}(m_b)]$	Observables	SM values
$\mathbf{C_7^{eff}}(\mu_\mathbf{b})$	$\mathcal{B}(\bar{B} \to X_s\gamma), A_I(B \to K^*\gamma), S_{K^*\gamma}, A_{FB}, F_L,$	-0.292
$\mathbf{C_9}(\mu_\mathbf{b})$	$\mathcal{B}(B \to X_s\ell\ell), A_{FB}, F_L,$	4.075
$\mathbf{C_{10}}(\mu_\mathbf{b})$	$\mathcal{B}(B_s \to \mu^+\mu^-), \mathcal{B}(B \to X_s\ell\ell), A_{FB}, F_L,$	-4.308
$\mathbf{C'_7}(\mu_\mathbf{b})$	$\mathcal{B}(\bar{B} \to X_s\gamma), A_I(B \to K^*\gamma), S_{K^*\gamma}, A_{FB}, F_L$	-0.006
$\mathbf{C'_9}(\mu_\mathbf{b})$	$\mathcal{B}(B \to X_s\ell\ell), A_{FB}, F_L$	0
$\mathbf{C'_{10}}(\mu_\mathbf{b})$	$\mathcal{B}(B_s \to \mu^+\mu^-), A_{FB}, F_L,$	0

More Precision Observables are necessary to overconstrain the deviations $\mathbf{C_i^{NP}}$

$\Rightarrow$ $B \to K^*(\to K\pi)\mu^+\mu^-$ can fulfill this requirement providing a set of large-recoil clean observables $\mathbf{P_{1,2,3}}, \mathbf{P'_{4,5,6,8}}$ and the corresponding CP observables $\mathbf{P^{CP}_{1,2,3}}, \mathbf{P^{CP\prime}_{4,5,6,8}}$

All those new observables $\mathbf{P_i}, \mathbf{P'_i}$ come from the angular distribution $\mathbf{\bar{B}_d} \to \mathbf{\bar{K}^{*0}}(\to \mathbf{K^-}\pi^+)\mathbf{l^+l^-}$ with the K^{*0} on the mass shell. It is described by $\mathbf{s} = \mathbf{q^2}$ and three angles θ_ℓ, $\theta_\mathbf{K}$ and ϕ

$$\frac{d^4\Gamma(\bar{B}_d)}{dq^2\, d\cos\theta_\ell\, d\cos\theta_K\, d\phi} = \frac{9}{32\pi}\mathbf{J}(\mathbf{q^2}, \theta_\ell, \theta_K, \phi) \quad \Rightarrow \quad \mathbf{f(J_{1s}, J_{1c}, J_{2s}, \ldots)}$$

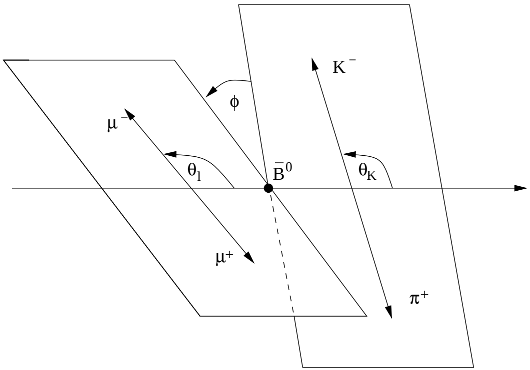

θ_ℓ: Angle of emission between $\bar{K}^{*0}$ and μ^- in di-lepton rest frame.
$\theta_\mathbf{K}$: Angle of emission between $\bar{K}^{*0}$ and K^- in di-meson rest frame.
ϕ: Angle between the two planes.

$\mathbf{q^2}$: dilepton invariant mass square.

Notice LHCb uses $\theta_\ell^{LHCb} = \pi - \theta_\ell^{us}$

Three regions in q^2:

- **low-q^2: large recoil for** K^*: $E_{K^*} \gg \Lambda_{QCD}$ or $\mathbf{4m_\ell^2} \leq \mathbf{q^2} < \mathbf{9}$ GeV^2
- resonance region ($q^2 = m^2_{J/\Psi}, \ldots$) betwen $9 < q^2 < 14$ GeV^2.
- **large-q^2: low-recoil for** K^*: $E_{K^*} \sim \Lambda_{QCD}$ or $\mathbf{14} < \mathbf{q^2} \leq (\mathbf{m_B} - \mathbf{m_{K^*}})^\mathbf{2}$.

Relation between J_i and P_j, P'_k observables

- The coefficients J_i contain transversity amplitudes $A_{\perp,\|,0}$ of the K^* which in turn

$$A_{\perp,\|,0} = (C_i^{SM} + \mathbf{C_i^{NP}}) \times \text{form factors}$$

$\Rightarrow$ *The cleanest procedure to separate the important Wilson Coefficient information from the Form Factor pollution is the use of P_i, P'_j observables*

The coefficients $\mathbf{J_i}$ of the distribution can be reexpressed now in terms of this basis of clean observables:

Correspondence $\mathbf{J_i} \leftrightarrow \mathbf{P_i^{(\prime)}}$:

BROWN: LO FF-dependent observables (F_L Longitudinal Polarization Fraction of K^*)

RED: LO FF-independent observables at large-recoil (defined from these eqs.)

Here for simplicity ($m_\ell = 0$). See [J.M'12] for $m_\ell \neq 0$.

$$(\mathbf{J_{2s}} + \mathbf{\bar{J}_{2s}}) = \frac{1}{4}\mathbf{F_T}\frac{\mathbf{d\Gamma + d\bar{\Gamma}}}{\mathbf{dq^2}} \qquad (\mathbf{J_{2c}} + \mathbf{\bar{J}_{2c}}) = -\mathbf{F_L}\frac{\mathbf{d\Gamma + d\bar{\Gamma}}}{\mathbf{dq^2}}$$

$$\mathbf{J_3} + \mathbf{\bar{J}_3} = \frac{1}{2}\mathbf{P_1}\mathbf{F_T}\frac{\mathbf{d\Gamma + d\bar{\Gamma}}}{\mathbf{dq^2}} \qquad \mathbf{J_3} - \mathbf{\bar{J}_3} = \frac{1}{2}\mathbf{P_1^{CP}}\mathbf{F_T}\frac{\mathbf{d\Gamma + d\bar{\Gamma}}}{\mathbf{dq^2}}$$

$$\mathbf{J_{6s}} + \mathbf{\bar{J}_{6s}} = 2\mathbf{P_2}\mathbf{F_T}\frac{\mathbf{d\Gamma + d\bar{\Gamma}}}{\mathbf{dq^2}} \qquad \mathbf{J_{6s}} - \mathbf{\bar{J}_{6s}} = 2\mathbf{P_2^{CP}}\mathbf{F_T}\frac{\mathbf{d\Gamma + d\bar{\Gamma}}}{\mathbf{dq^2}}$$

$$\mathbf{J_9} + \mathbf{\bar{J}_9} = -\mathbf{P_3}\mathbf{F_T}\frac{\mathbf{d\Gamma + d\bar{\Gamma}}}{\mathbf{dq^2}} \qquad \mathbf{J_9} - \mathbf{\bar{J}_9} = -\mathbf{P_3^{CP}}\mathbf{F_T}\frac{\mathbf{d\Gamma + d\bar{\Gamma}}}{\mathbf{dq^2}}$$

$$\mathbf{J_4} + \mathbf{\bar{J}_4} = \frac{1}{2}\mathbf{P'_4}\sqrt{\mathbf{F_T F_L}}\frac{\mathbf{d\Gamma + d\bar{\Gamma}}}{\mathbf{dq^2}} \qquad \mathbf{J_4} - \mathbf{\bar{J}_4} = \frac{1}{2}\mathbf{P_4^{\prime CP}}\sqrt{\mathbf{F_T F_L}}\frac{\mathbf{d\Gamma + d\bar{\Gamma}}}{\mathbf{dq^2}}$$

$$\mathbf{J_5} + \mathbf{\bar{J}_5} = \mathbf{P'_5}\sqrt{\mathbf{F_T F_L}}\frac{\mathbf{d\Gamma + d\bar{\Gamma}}}{\mathbf{dq^2}} \qquad \mathbf{J_5} - \mathbf{\bar{J}_5} = \mathbf{P_5^{\prime CP}}\sqrt{\mathbf{F_T F_L}}\frac{\mathbf{d\Gamma + d\bar{\Gamma}}}{\mathbf{dq^2}}$$

$$\mathbf{J_7} + \mathbf{\bar{J}_7} = -\mathbf{P'_6}\sqrt{\mathbf{F_T F_L}}\frac{\mathbf{d\Gamma + d\bar{\Gamma}}}{\mathbf{dq^2}} \qquad \mathbf{J_7} - \mathbf{\bar{J}_7} = -\mathbf{P_6^{\prime CP}}\sqrt{\mathbf{F_T F_L}}\frac{\mathbf{d\Gamma + d\bar{\Gamma}}}{\mathbf{dq^2}}$$

How do we know that we have a complete description for $B \to K^*(\to K\pi)\mu^+\mu^-$

[Egede, Hurth, JM, Ramon, Reece'10]

An important step forward was the identification of the **symmetries** of the distribution:

Transformation of amplitudes leaving distribution invariant.

Symmetries determine the minimal # observables for each scenario:

$$n_{obs} = 2n_A - n_S$$

Case	Coefficients	Amplitudes	Symmetries	Observables
$m_\ell = 0,\ A_S = 0$	11	6	4	**8**
$m_\ell = 0$	11	7	5	**9**
$m_\ell > 0,\ A_S = 0$	11	7	4	**10**
$m_\ell > 0$	12	8	4	**12**

All symmetries (massive and scalars) were found explicitly later on.

[JM, Mescia, Ramon, Virto'12]

Symmetries $\Rightarrow$ # of observables $\Rightarrow$ determine a **basis**: each angular observable constructed can be expressed in terms of this basis.

P_i, P_i' defines an **Optimal Basis** of observables, a compromise between:

- *Excellent experimental accessibility and simplicity of the fit.*
- *Reduced FF dependence (in the large-recoil region:* $0.1 \leq q^2 \leq 9\ \mathrm{GeV}^2$).

Our proposal for **CP-conserving basis**:

$$\left\{ \frac{\mathbf{d\Gamma}}{\mathbf{dq^2}}, \mathbf{A_{FB}}, \mathbf{P_1}, \mathbf{P_2}, \mathbf{P_3}, \mathbf{P_4'}, \mathbf{P_5'}, \mathbf{P_6'} \right\} \text{ or } \mathbf{P_3} \leftrightarrow \mathbf{P_8'} \text{ and } \mathbf{A_{FB}} \leftrightarrow \mathbf{F_L}$$

where $P_1 = A_T^2$ [Kruger, J.M'05],
$P_2 = \frac{1}{2} A_T^{\rm re}, P_3 = -\frac{1}{2} A_T^{\rm im}$ [Becirevic, Schneider'12]
$P'_{4,5,6}$ [Descotes, JM, Ramon, Virto'13]).

The corresponding **CP-violating basis** ($J_i + \bar{J}_i \to J_i - \bar{J}_i$ in numerators):

$$\left\{ \mathbf{A_{CP}}, \mathbf{A_{FB}^{CP}}, \mathbf{P_1^{CP}}, \mathbf{P_2^{CP}}, \mathbf{P_3^{CP}}, \mathbf{P_4^{\prime CP}}, \mathbf{P_5^{\prime CP}}, \mathbf{P_6^{\prime CP}} \right\} \text{ or } \mathbf{P_3^{CP}} \leftrightarrow \mathbf{P_8^{\prime CP}} \text{ and } \mathbf{A_{FB}^{CP}} \leftrightarrow \mathbf{F_L^{CP}}$$

P_1 and P_2 observables function of $A_\perp$ and $A_\parallel$ amplitudes

- **P_1**: Proportional to $|A_\perp|^2 - |A_\parallel|^2$
  - Test the LH structure of SM and/or existence of RH currents that breaks $A_\perp \sim -A_\parallel$
- **P_2**: Proportional to $\mathrm{Re}(A_i A_j)$
  - Zero of P_2 at the same position as the zero of A_{FB}
  - P_2 is the clean version of A_{FB}. Their different normalizations offer different sensitivities.

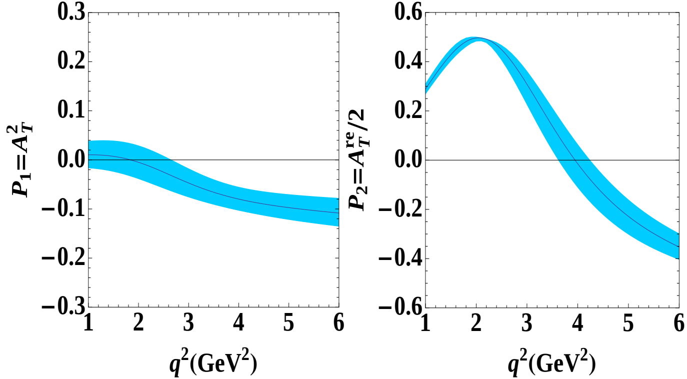

- P_3 and $P'_{6,8}$ are proportional to $\mathrm{Im} A_i A_j$ and small if there are no large phases. All are < 0.1.
- P_i^{CP} are all negligibly small if there is no New Physics in weak phases.

P_4' and P_5' observables function of $A_{\perp,\|}$ and also A_0 amplitudes

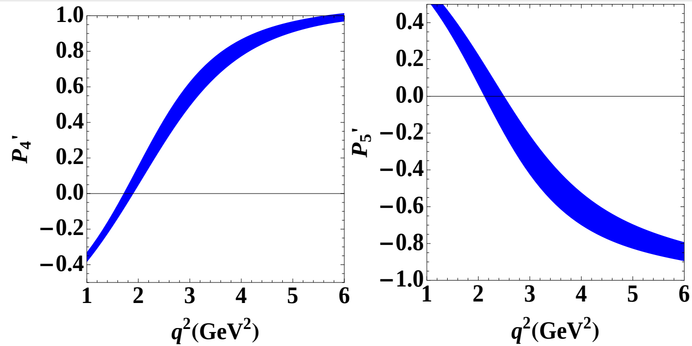

- $\mathbf{P'_{4,5}}$: Proportional to $\mathrm{Re}(A_i A_j)$
- $|P_{4,5}| \leq 1$ but $|P'_{4,5}|$ can be > 1.

In the large-recoil limit

$$A^L_{\perp,\|} \propto \left[\mathcal{C}_9^{\rm eff} - \mathcal{C}_{10} + \frac{2\hat{m}_b}{\hat{s}}\mathcal{C}_7^{\rm eff}\right]\xi_\perp(E_{K^*}) \qquad A^R_{\perp,\|} \propto \left[\mathcal{C}_9^{\rm eff} + \mathcal{C}_{10} + \frac{2\hat{m}_b}{\hat{s}}\mathcal{C}_7^{\rm eff}\right]\xi_\perp(E_{K^*})$$

$$A^L_0 \propto \left[\mathcal{C}_9^{\rm eff} - \mathcal{C}_{10} + 2\hat{m}_b\mathcal{C}_7^{\rm eff}\right]\xi_\|(E_{K^*}) \quad A^R_0 \propto \left[\mathcal{C}_9^{\rm eff} + \mathcal{C}_{10} + 2\hat{m}_b\mathcal{C}_7^{\rm eff}\right]\xi_\|(E_{K^*})$$

- In the SM $C_9^{SM} \sim -C_{10}^{SM}$, this cancellation strongly suppresses $A^R_{\perp,\|}$ above 4 Gev^2: $A^L_{\perp,\|} >> A^R_{\perp,\|}$. This makes $P_4 \to 1$ and $P_5 \to -1$ for $q^2 \to 8$ GeV^2 quite fast BUT the fact that $|A_\|| > |A_\perp|$ and that $P_4' \propto A_0^{L*}A_\|^L + A_0^R A_\|^{R*}$ and $P_5' \propto A_0^{L*}A_\perp^L - A_0^R A_\perp^{R*}$ makes less efficient the convergence in the case of P_5'.
- In presence of New Physics affecting only C_9 the cancellation $C_9 \sim -C_{10}$ is less efective, consequently $A^R_{\perp,\|}$ is less suppressed and one should expect to see the effect of $C_9 \neq C_9^{SM}$ in P_5'.

Analysis of new LHCb data on

$$B \to K^* \mu^+ \mu^-$$

Experimental evidence: EPS+ Beauty

Present bins: [0.1,2], [2,4.3], [4.3,8.68], [1,6], [14.18,16], [16,19] GeV^2.

Observable	Experiment	SM prediction	Pull
$\langle P_1 \rangle_{[0.1,2]}$	$-0.19^{+0.40}_{-0.35}$	$0.007^{+0.043}_{-0.044}$	-0.5
$\langle P_1 \rangle_{[2,4.3]}$	$-0.29^{+0.65}_{-0.46}$	$-0.051^{+0.046}_{-0.046}$	-0.4
$\langle P_1 \rangle_{[4.3,8.68]}$	$0.36^{+0.30}_{-0.31}$	$-0.117^{+0.056}_{-0.052}$	$+1.5$
$\langle P_1 \rangle_{[1,6]}$	$0.15^{+0.39}_{-0.41}$	$-0.055^{+0.041}_{-0.043}$	$+0.5$
$\langle P_2 \rangle_{[0.1,2]}$	$0.03^{+0.14}_{-0.15}$	$0.172^{+0.020}_{-0.021}$	-1.0
$\langle P_2 \rangle_{[2,4.3]}$	$0.50^{+0.00}_{-0.07}$	$0.234^{+0.060}_{-0.086}$	**$+2.9$**
$\langle P_2 \rangle_{[4.3,8.68]}$	$-0.25^{+0.07}_{-0.08}$	$-0.407^{+0.049}_{-0.037}$	**$+1.7$**
$\langle P_2 \rangle_{[1,6]}$	$0.33^{+0.11}_{-0.12}$	$0.084^{+0.060}_{-0.078}$	$+1.8$
$\langle A_{\rm FB} \rangle_{[0.1,2]}$	$-0.02^{+0.13}_{-0.13}$	$-0.136^{+0.051}_{-0.048}$	$+0.8$
$\langle A_{\rm FB} \rangle_{[2,4.3]}$	$-0.20^{+0.08}_{-0.08}$	$-0.081^{+0.055}_{-0.069}$	-1.1
$\langle A_{\rm FB} \rangle_{[4.3,8.68]}$	$0.16^{+0.06}_{-0.05}$	$0.220^{+0.138}_{-0.113}$	-0.5
$\langle A_{\rm FB} \rangle_{[1,6]}$	$-0.17^{+0.06}_{-0.06}$	$-0.035^{+0.037}_{-0.034}$	-2.0

- **$\mathbf{P_1}$**: No substantial deviation (large error bars).
- **$\mathbf{A_{\rm FB}}$-$\mathbf{P_2}$**: A slight tendency for a lower value of the second and third bins of $A_{\rm FB}$ is consistent with a $2.9\,\sigma$ ($1.7\,\sigma$) deviation in the second (third) bin of P_2.
- **Zero**: Preference for a slightly higher q^2-value for the zero of $A_{\rm FB}$ (same as the zero of P_2).

Both effects can be accommodated with $\mathcal{C}_7^{\rm NP} < 0$ and/or $\mathcal{C}_9^{\rm NP} < 0$.

Experimental evidence: EPS+ Beauty

Observable	Experiment	SM prediction	Pull
$\langle P_4' \rangle_{[0.1,2]}$	$0.00^{+0.52}_{-0.52}$	$-0.342^{+0.031}_{-0.026}$	$+0.7$
$\langle P_4' \rangle_{[2,4.3]}$	$0.74^{+0.54}_{-0.60}$	$0.569^{+0.073}_{-0.063}$	$+0.3$
$\langle P_4' \rangle_{[4.3,8.68]}$	$1.18^{+0.26}_{-0.32}$	$1.003^{+0.028}_{-0.032}$	$+0.6$
$\langle P_4' \rangle_{[1,6]}$	$0.58^{+0.32}_{-0.36}$	$0.555^{+0.067}_{-0.058}$	$+0.1$
$\langle P_5' \rangle_{[0.1,2]}$	$0.45^{+0.21}_{-0.24}$	$0.533^{+0.033}_{-0.041}$	-0.4
$\langle P_5' \rangle_{[2,4.3]}$	$0.29^{+0.40}_{-0.39}$	$-0.334^{+0.097}_{-0.113}$	$\mathbf{+1.6}$
$\langle P_5' \rangle_{[4.3,8.68]}$	$-0.19^{+0.16}_{-0.16}$	$-0.872^{+0.053}_{-0.041}$	$\mathbf{+4.0}$
$\langle P_5' \rangle_{[1,6]}$	$0.21^{+0.20}_{-0.21}$	$-0.349^{+0.088}_{-0.100}$	$+2.5$
$\langle P_4' \rangle_{[14.18,16]}$	$-0.18^{+0.54}_{-0.70}$	$1.161^{+0.190}_{-0.332}$	-2.1
$\langle P_4' \rangle_{[16,19]}$	$0.70^{+0.44}_{-0.52}$	$1.263^{+0.119}_{-0.248}$	-1.1
$\langle P_5' \rangle_{[14.18,16]}$	$\mathbf{-0.79^{+0.27}_{-0.22}}$	$\mathbf{-0.779^{+0.328}_{-0.363}}$	$+0.0$
$\langle P_5' \rangle_{[16,19]}$	$\mathbf{-0.60^{+0.21}_{-0.18}}$	$\mathbf{-0.601^{+0.282}_{-0.367}}$	$+0.0$

Definition of the anomaly:

- $\mathbf{P_5'}$: There is a striking $4.0\,\sigma$ ($1.6\,\sigma$) deviation in the third (second) bin of P_5'.

  Consistent with large negative contributions in $\mathcal{C}_7^{\rm NP}$ and/or $\mathcal{C}_9^{\rm NP}$.

- $\mathbf{P_4'}$: in agreement with the SM, but within large uncertainties, and it has future potential to determine the sign of $\mathcal{C}_{10}^{\rm NP}$.

- $\mathbf{P_6'}$ and $\mathbf{P_8'}$: show small deviations with respect to the SM, but such effect would require complex phases in $\mathcal{C}_9^{\rm NP}$ and/or $\mathcal{C}_{10}^{\rm NP}$.

Us: $(-0.19-(-0.872))/\sqrt{0.16^2+0.053^2}=4.05$ and **Exp**: $(-0.19-(-0.872+0.053))/\sqrt{0.16^2+0.053^2}=3.73$

Our SM predictions+LHCb data

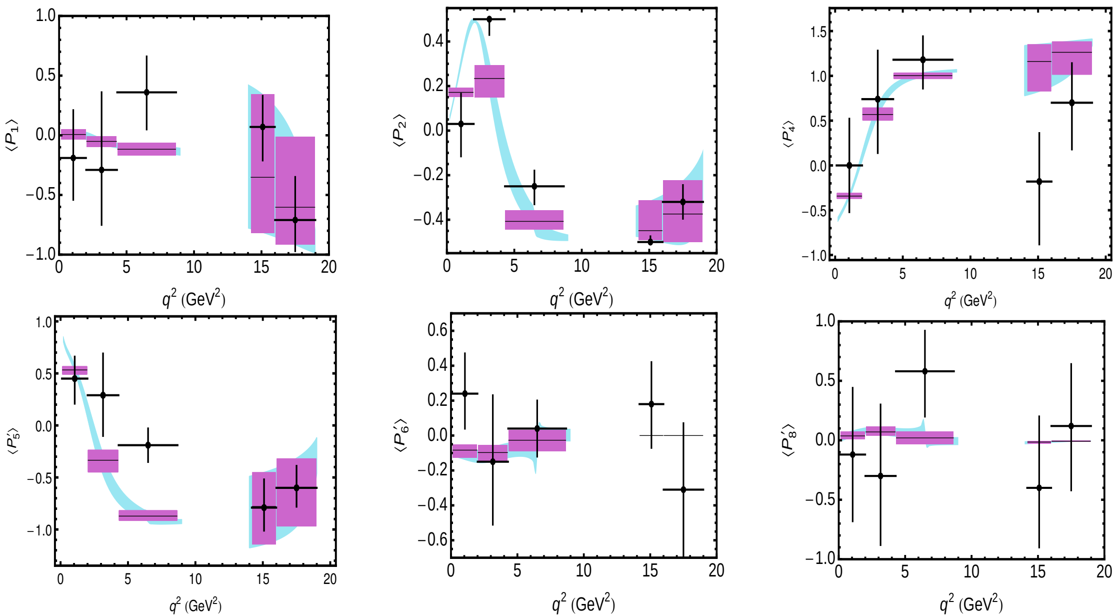

Figure : Experimental measurements and SM predictions for some $B \to K^* \mu^+ \mu^-$ observables. The black crosses are the experimental LHCb data. The blue band corresponds to the SM predictions for the differential quantities, whereas the purple boxes indicate the corresponding binned observables.

Description of the analysis

Goal: Determine the Wilson coefficients $\mathcal{C}_{7,9,10}$, $\mathcal{C}'_{7,9,10}$: $\mathcal{C}_i = \mathcal{C}_i^{SM} + \mathcal{C}_i^{NP}$

Standard χ^2 frequentist approach: Asymmetric errors included, estimate theory uncertainties for each set of $\mathcal{C}_i^{NP}$ and all uncertainties are combined in quadrature.

IMPORTANT: *Experimental correlations are included in the updated plot*

We do three analysis: a) large-recoil data b) large+low-recoil data c) [1-6] bin

Observables:

- $B \to K^* \mu^+ \mu^-$: We take observables P_1, P_2, P_4', P_5', P_6' and P_8' in the following binning:
  - -**large-recoil**: $[0.1, 2], [2, 4.3], [4.3, 8.68]$ GeV^2.
  - -**low recoil**: [14.18,16], [16,19] GeV^2
  - -**wide large-recoil bin**: $[1, 6]$ GeV^2.

- Radiative and dileptonic B decays: $\mathcal{B}(B \to X_s \gamma)_{E_\gamma > 1.6\mathrm{GeV}}$, $\mathcal{B}(B \to X_s \mu^+ \mu^-)_{[1,6]}$ and $\mathcal{B}(B_s \to \mu^+ \mu^-)$, $A_I(B \to K^* \gamma)$ and the $B \to K^* \gamma$ time-dependent CP asymmetry $S_{K^* \gamma}$

General case all WC free

Result of our analysis (large+low recoil data+rad) if we allow **all Wilson coefficients** to vary freely:

Coefficient	1σ	2σ	3σ
$\mathcal{C}_7^{\rm NP}$	$[-0.05,-0.01]$	$[-0.06, 0.01]$	$[-0.08, 0.03]$
$\mathcal{C}_9^{\rm NP}$	$[-1.6,-0.9]$	$[-1.8,-0.6]$	$[-2.1,-0.2]$
$\mathcal{C}_{10}^{\rm NP}$	$[-\mathbf{0.4}, \mathbf{1.0}]$	$[-1.2, 2.0]$	$[-2.0, 3.0]$
$\mathcal{C}_{7'}^{\rm NP}$	$[-\mathbf{0.04}, \mathbf{0.02}]$	$[-0.09, 0.06]$	$[-0.14, 0.10]$
$\mathcal{C}_{9'}^{\rm NP}$	$[-0.2, 0.8]$	$[-0.8, 1.4]$	$[-1.2, 1.8]$
$\mathcal{C}_{10'}^{\rm NP}$	$[-\mathbf{0.4}, \mathbf{0.4}]$	$[-1.0, 0.8]$	$[-1.4, 1.2]$

Table : 68.3% (1σ), 95.5% (2σ) and 99.7% (3σ) confidence intervals for the NP contributions to WC.

This table tells you again that there is **strong evidence for a $\mathcal{C}_9^{\rm NP} < 0$, preference for $\mathcal{C}_7^{\rm NP} < 0$** and **no clear-cut evidence** for $\mathcal{C}_{10,7',9',10'}^{\rm NP} \neq 0$.

This does not imply that they will be at the end zero but that **present data** *does not point clearly for a positive or negative value.*

In conclusion our pattern of [PRD88 (2013) 074002] is

$$\mathbf{C_9^{NP}} \sim [-\mathbf{1.6}, -\mathbf{0.9}], \quad \mathbf{C_7^{NP}} \sim [-\mathbf{0.05}, -\mathbf{0.01}], \quad \mathbf{C_9'} \sim \pm\delta \quad \mathbf{C_{10}}, \mathbf{C'_{7,10}} \sim \pm\epsilon$$

where δ is small (at maximum half $|\mathbf{C_9^{NP}}|$) and ϵ is smaller. **A simplified version is** $C_9^{NP} = -1.5$

Best fit points: **(too large)**

Large recoil: $\mathbf{C_9^{NP}} = -\mathbf{1.6}$, $C_{10}^{\rm NP} = +0.2$, $C_7^{\rm NP} = -0.02$, $\mathbf{C_{9'}^{NP}} = -\mathbf{1.4}$, $C_{7'}^{\rm NP} = +0.005$, $C_{10'}^{\rm NP} = -0.13$.
Large+Low: $\mathbf{C_9^{NP}} = -\mathbf{1.2}$, $C_{10}^{\rm NP} = +0.4$, $C_7^{\rm NP} = -0.03$, $\mathbf{C_{9'}^{NP}} = +\mathbf{0.4}$, $C_{7'}^{\rm NP} = -0.012$, $C_{10'}^{\rm NP} = -0.04$

Branching Ratio of $B \to K^* \mu^+ \mu^-$

Let's look now to one observables strongly dependent on FF the BR $(x10^7)$ that we use as cross check.

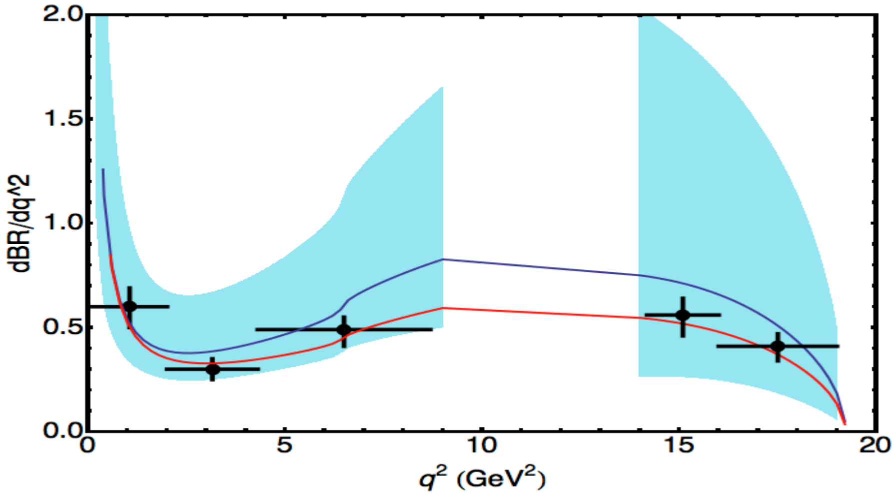

where the blue curve is SM and the red curve corresponds to $C_9^{NP} = -1.5$. Interestingly the central value goes in the right direction, but given the error bars all is consistent with data.

Updated result with experimental correlations

Updated result using $\mathbf{P_i}, \mathbf{P'_i}, \mathbf{A}_{\rm FB}$ and **experimental correlations**.

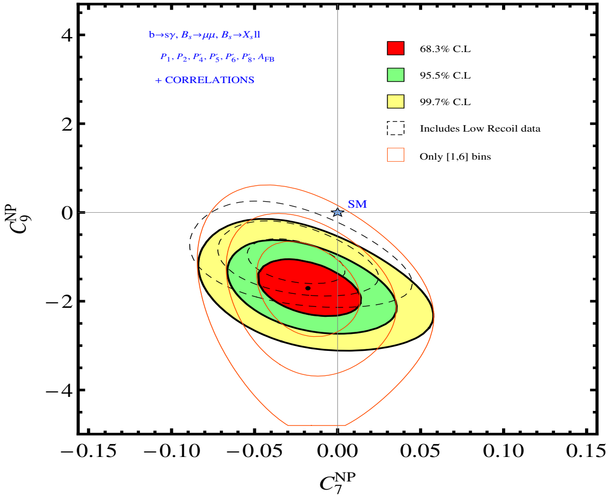

From the analysis of the set $\mathbf{P_i}, \mathbf{P'_i}, \mathbf{A}_{\rm FB}+$ **BR** + exp. correlations we get:

4.3σ (large-recoil)
3.6σ (large + low recoil)
2.8σ for [1-6] bin.

Colored: large-recoil and
dashed: large+low recoil
orange: [1-6] bin

- We checked (for completeness) that we find **same significance** using $\mathbf{P_i}, \mathbf{P'_i}, \mathbf{F_L}$ instead of $\mathbf{A}_{\rm FB}$.
  Positive: **Our SM $\mathbf{F_L}$** fully compatible with all data (not only LHCb) and less correlated.
  Negative: Result using F_L is less solid than using A_{FB} since it depends on choice of FF.

We are further refining the theoretical analysis, in couple of months we will update it.

The simplified best fit point $C_9^{NP} = -1.5$ (in red) for the relevant observables.

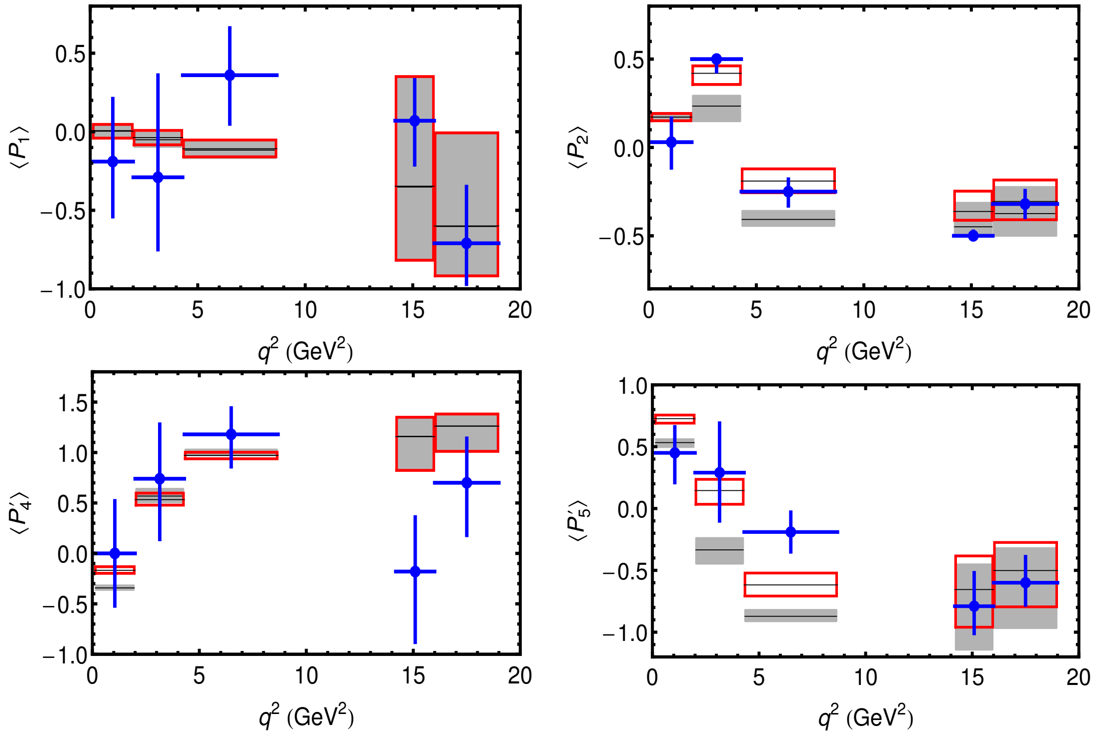

Recent measurements of the decay channel $B^+ \to K^+\mu^+\mu^-$ has shown different peaking structures in the dimuon spectrum in the low-recoil region $q^2 > 16$ GeV^2.

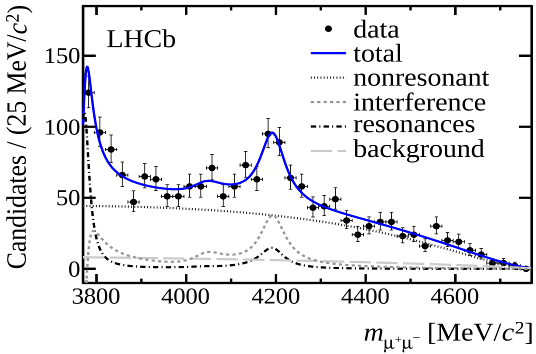

This is due to the interference of this decay mode with at least the $\psi(4160)$ resonance. Other resonances are less clear in significance but also there.

This kind of peaking structure it is expected also in $B \to K^*\mu^+\mu^-$, consequently, predictions and information from low-recoil region has to be taken with extreme caution.

Can we test if the anomaly in P_5' is isolated?

Answer:

We should wait for 3 fb^{-1} data

BUT

already now there are interesting hints...

[Egede, Hurth, JM, Ramon, Reece JHEP 1010 (2010) 056]

Let's review first the **symmetry formalism** for the massless angular distribution:

$$\mathbf{n}_{\|} = \begin{pmatrix} A_{\|}^L \\ A_{\|}^{R*} \end{pmatrix}, \quad \mathbf{n}_{\perp} = \begin{pmatrix} A_{\perp}^L \\ -A_{\perp}^{R*} \end{pmatrix}, \quad \mathbf{n_0} = \begin{pmatrix} A_0^L \\ A_0^{R*} \end{pmatrix}.$$

All the coefficients $\mathbf{J_i}$ can be expressed in terms of the products $\mathbf{n_i^\dagger}\, \mathbf{n_j}$ (example):

$$J_3 = \frac{1}{2}\left(|n_\perp|^2 - |n_\||^2\right), \quad J_4 = \frac{1}{\sqrt{2}}\mathrm{Re}(n_0^\dagger\, n_\|), \quad J_5 = \sqrt{2}\,\mathrm{Re}(n_0^\dagger\, n_\perp), \quad J_9 = -\mathrm{Im}(n_\perp^\dagger\, n_\|)$$

A **symmetry** of the angular distribution will be a unitary transformation $n_i \to U n_i$

$$n_i' = U n_i = \begin{bmatrix} e^{i\phi_L} & 0 \\ 0 & e^{-i\phi_R} \end{bmatrix} \begin{bmatrix} \cos\theta & -\sin\theta \\ \sin\theta & \cos\theta \end{bmatrix} \begin{bmatrix} \cosh i\tilde{\theta} & -\sinh i\tilde{\theta} \\ -\sinh i\tilde{\theta} & \cosh i\tilde{\theta} \end{bmatrix} n_i\,.$$

U defines the **four symmetries** of the massless angular distribution:

- two global phase transformations (ϕ_L and ϕ_R),
- a rotation θ among the real and imaginary components of the amplitudes independently
- another rotation $\tilde{\theta}$ that mixes real and imaginary components of the transversity amplitudes.

Solving the system of equations of $A_{\perp,\|,0}$ in terms of J_i (using three of the symmetries) we found:

$$e^{i(\phi_0^{\mathbf{L}}-\phi_\perp^{\mathbf{L}})} = \frac{2(2J_{2s}-J_3)(J_5+2iJ_8)-(2J_4+iJ_7)(J_{6s}-2iJ_9)}{\sqrt{16J_{2s}^2-4J_3^2-J_{6s}^2-4J_9^2}\sqrt{2J_{1c}(2J_{2s}-J_3)-4J_4^2-J_7^2}},$$

This equation is related to the freedom associated to the **fourth** unused symmetry transformation $\tilde{\theta}$.

Imposing that its modulo is one we find:

$$J_{2c} = -2\frac{(2J_{2s}+J_3)\left(4J_4^2+\beta_\ell^2 J_7^2\right)+(2J_{2s}-J_3)\left(\beta_\ell^2 J_5^2+4J_8^2\right)}{16J_{2s}^2-\left(4J_3^2+\beta_\ell^2 J_{6s}^2+4J_9^2\right)} + 4\frac{\beta_\ell^2 J_{6s}(J_4J_5+J_7J_8)+J_9(\beta_\ell^2 J_5J_7-4J_4J_8)}{16J_{2s}^2-\left(4J_3^2+\beta_\ell^2 J_{6s}^2+4J_9^2\right)},$$

Indeed an identical equation can be written in terms of the $\bar{J}_i$.

[J.M, N. Serra '14]

This equation can be expressed in terms of P_i and P_i^{CP} observables to get:

$$\bar{P}_2 = +\frac{1}{2\bar{k}_1}\left[(\bar{P}_4'\bar{P}_5' + \delta_1) + \frac{1}{\beta}\sqrt{(-1+\bar{P}_1+\bar{P}_4'^2)(-1-\bar{P}_1+\beta^2\bar{P}_5'^2)+\delta_2+\delta_3\bar{P}_1+\delta_4\bar{P}_1^2}\right]$$

where

$$\bar{P}_i = P_i + P_i^{CP} \qquad \beta = \sqrt{1-4m_\ell^2/s}$$

The sign in front of the square root is taken "+" everywhere by comparison with exact result in SM, at low-recoil both solutions (+ and -) converge. (Plot with $\delta_i \to 0$)

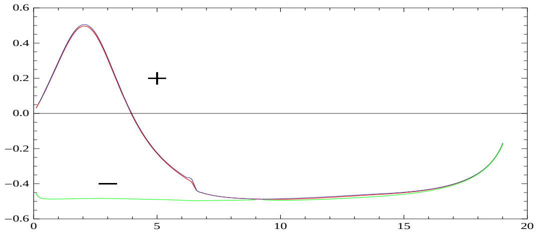

REMARK:

- **This is an exact equation valid for any q^2 (low, large) and obtained from symmetries.**
- **It involves 6 P_i of the basis plus one redundant.**

An identical equation can be written in terms of $\hat{P}_i = P_i - P_i^{CP}$, substituting $\bar{P}_i \to \hat{P}_i$ everywhere. More importantly all terms inside the δ_i are strongly suppressed (by small strong and weak phases):

$$\delta_i \sim \mathcal{O}((\mathrm{Im}A_i)^2, 1-\bar{k}_1) \quad \text{and} \quad \bar{k}_1 = 1 + F_L^{CP}/F_L$$

Hypothesis: No **New Physics in weak phases** entering Wilson coefficients and **not scalars/tensors**. Both hypothesis can be tested, measuring P_i^{CP} and S_1.

To an **excellent approximation** we have:

$$P_2 = \frac{1}{2}\left[P'_4 P'_5 + \frac{1}{\beta}\sqrt{(-1 + P_1 + P'^2_4)(-1 - P_1 + \beta^2 P'^2_5)}\right]$$

This equation can be used in *binned form* if:

- Observables are nearly constant inside the bin
- Or the size of the bin is very small.

We correct for this by $\langle P_2 \rangle \to \langle P_2 \rangle + \Delta^{\rm NP}_{\rm exact-relation}$ where $\Delta^{\rm NP}_{\rm exact-relation}$ is order 10^{-2} except for [0.1-2] bin and [1-6] bin.

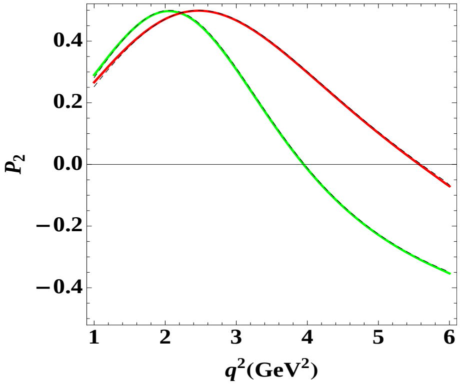

Figure : Green: SM exact, dashed inside approximation, Red: NP $C_9^{NP} = -1.5$ exact, dashed inside approximation

- The terms δ_i has been computed in the SM and in presence of New Physics [constrained range] being always bounded within $10^{-1} - 10^{-2}$.

The striking consequence of this equation is that it allows you to use data **to predict** *the* **impact of the anomaly in** P'_5 *in a completely* **different observable***:* P_2

Implication I: **A new bound on** P_1

Imposing that the square root is well defined one finds:

$$P_5'^2 - 1 \leq P_1 \leq 1 - P_4'^2$$

- Indeed this is an exact bound that could be alternatively obtained from

$$|P_4| = |P_4'|/\sqrt{1-P_1} \leq 1 \quad \text{and} \quad |P_5| = |P_5'|/\sqrt{1+P_1} \leq 1$$

$|P_{4,5}| \leq 1$ comes from the geometrical interpretation of those observables in terms of n_i.

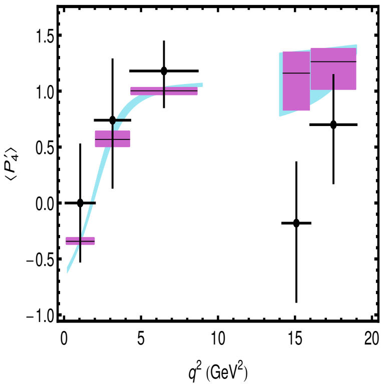

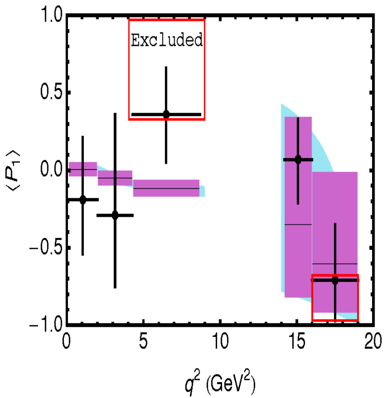

- The new upper bound is very stringent for the [4.3,8.68] bin, cutting most of the space for a positive P_1: $P_1^{[4.3,8.68]} < 0.33$
- The lower bound is particularly relevant for the [16,19] bin of P_1: $P_1^{[16,19]} > -0.68$.

Implication II: **At the position of the zero q_0^2 of P_2 (same as A_{FB}) the following relation holds:**

$$[P_4^2 + P_5^2]|_{q^2=q_0^2} = 1 \quad \text{or} \qquad [P_4'^2 + P_5'^2]|_{q^2=q_0^2} = 1 - \eta(q_0^2)$$

where

$$\eta(q_0^2) = P_1^2 + P_1(P_4'^2 - P_5'^2)|_{q^2=q_0^2}$$

SM Zero of A_{FB}: $q_0^{2SM} = 3.95 \pm 0.38$ (our), 3.90 ± 0.12 (Buras'08), 2.9 ± 0.3 (Khodjamirian'10) GeV^2
Experimental LHCb data: $q_0^{2LHCb} = 4.9 \pm 0.9$ GeV^2

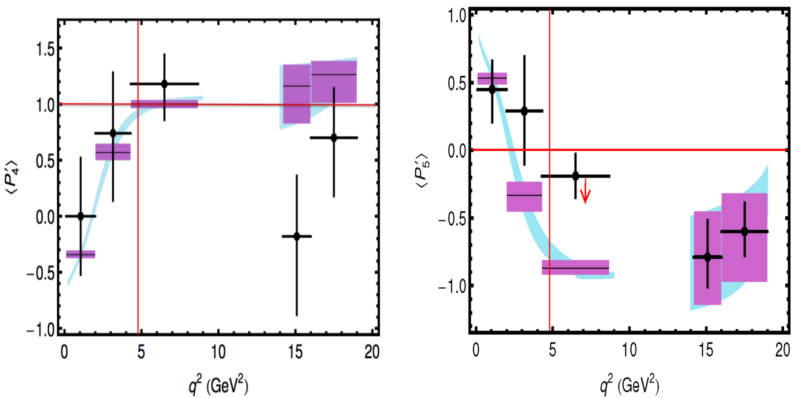

Assume that a future precise measurement of the zero confirms $q_0^{2exp} \sim 4.9$ GeV^2 with small error.

If $P_4' \sim 1$ and $P_1 \geq 0$ at $q_0^2 = 4.9$ GeV^2 (like present data seems to suggest) then one should find $P_1(q_0^2) \leq 1 - P_4'^2 \sim 0$, $\eta(q_0^2) \sim 0$ **and** $\mathbf{P_5'(q_0^2) \sim 0}$

(notice that in SM $P_5'(q_0^2) = -0.75$)

A precise measurement of q_0^2 (zero of A_{FB}) outside the SM region would serve as an indirect confirmation of the anomaly

Implication III: **We can establish a new relation between the anomaly bin in P_5' and P_2:**

$$\langle P_2\rangle = \frac{1}{2}\left[\langle P_4'\rangle\langle P_5'\rangle + \sqrt{(-1+\langle P_1\rangle+\langle P_4'\rangle^2)(-1-\langle P_1\rangle+\langle P_5'\rangle^2)}\right] + \Delta_{exact}^{bin}$$

where $\Delta_{exact}^{bin} = -0.04$ for NP best fit point at 2nd and 3rd bin, while $\Delta_{exact}^{bin} = -0.01$ for 1 GeV^2 size.

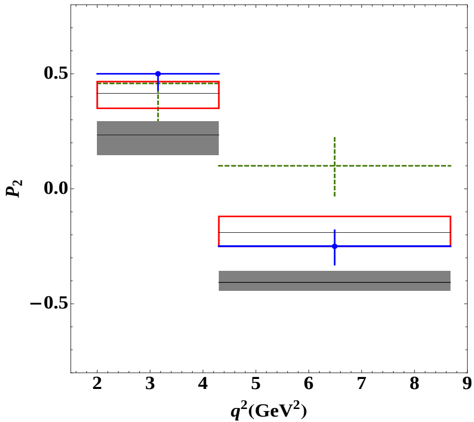

GRAY band: SM prediction. **BLUE cross**: Measured value of P_2
RED rectangle: $C_9^{NP} = -1.5$ NP prediction.
Green cross is $\langle P_2\rangle$ obtained from combining data of $\langle P_{4,5}'\rangle$, $\langle P_1\rangle$, considering asymmetric errors and bound on P_1

- Bin [2,4.3]: LHCb data:$+0.50^{+0}_{-0.07}$,Relation:$+0.46^{+0}_{-0.19}$
  0.2σ measured (blue cross) versus relation (green cross)
- Bin[4.3,8.68]: LHCb data:$-0.25^{+0.07}_{-0.08}$, Relation:$+0.10^{+0.13}_{-0.13}$
  2.4σ measured (blue cross) versus relation (green cross),
  1.9σ from relation to NP best fit point (red box),
  3.6σ from relation to SM.

Extremely simplified where $P_4' \sim 1$ (if $P_1 \sim 0$): $P_2 \sim \frac{1}{2}P_5'$

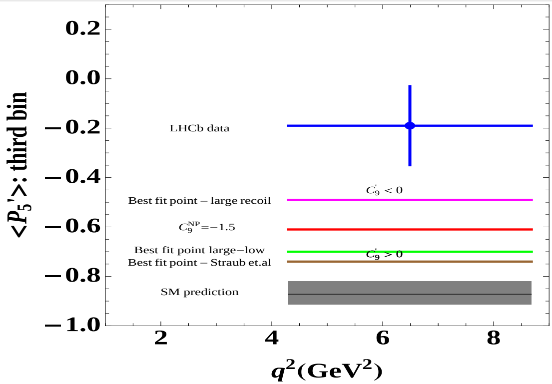

It is not surprising that the second bin in P_2 fits perfectly, while the third bin in P_2 is on the right direction but not perfect.

Reason It is very difficult to get excellent agreement with the third bin of P_5' inside a global fit.

- Our best fit point obtained from large-recoil data is $(C_7^{NP}, C_9^{NP}, C_{10}^{NP}, C_7', C_9', C_{10}') = (-0.02, -1.6, +0.18, +0.005, -1.4, -0.13)$ gives $\langle P_5' \rangle_{[4.3,8.68]} = -0.49$ and reduces tension with data -0.19 ± 0.16 at 1.8σ.
- The best fit point with $C_9^{NP} = -1.5$ gives $\langle P_5' \rangle_{[4.3,8.68]} = -0.61$
- The best fit point from Altmannshofer & Straub gives $\langle P_5' \rangle_{[4.3,8.68]} = -0.74$ in much worst disagreement with data. Same problem applies to Hambrock et al.'13 and Bobeth et al'13 (they all missed the 3-bin information and naturally got a wrong bias in favor of a large positive C_9').
  S. Meinel [private communication] extrapolated lattice results to large-recoil and agree with us.

Most plausible scenario: Third bin in P_5' will go down (reducing distance with SM) while third bin in P_2 might go up (enlarging distance with SM): *Global picture much more consistent.*

Implication IV: **The first low-recoil bin [14.18,16] can also be tested using this equation**

LHCb data on P_2 in this bin gives: $-\mathbf{0.50}^{+0.03}_{-0.00}$

LHCb data on P'_4, P_1, P'_5 implies that P_2 should be: $+\mathbf{0.50}^{+0}_{-0.27}$ (if +) or $-\mathbf{0.50}^{+0.33}_{+0}$ (if -)

This shows a discrepancy of **3.7**σ (if +) or agreement (if -) but both solutions + and - should give same result at low-recoil $\Rightarrow$ probably a statistical fluctuation or a problem at low recoil

Implication V: ALTERNATIVELY **Full fit of the angular distribution with a small dataset**

Under the assumption of real Wilson coefficients one has

- Free parameters F_L, P_1, $P'_{4,5}$.
- P_2 is a function of the other observables and $P'_{6,8}$ are set to zero.

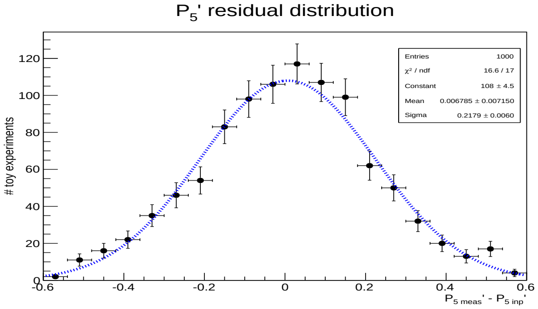

Figure : Residual distribution of P'_5 when fitting with 100 events. The fit of a gaussian distribution is superimosed.

We find testing this fit for values around the measured values: **convergence and unbiased pulls** with as little as 50 events per bin. Gaussian pulls are obtained with only 100 events.

This opens the possibility to perform a full angular fit analysis with small bins in q^2

The main hypothesis (real WC) can be tested measuring P_i^{CP}.

Explanation of the controversy about size and sign of C_9'

Our pattern: $\mathbf{C_9^{NP}} \sim [-\mathbf{1.6}, -\mathbf{0.9}]$, $\mathbf{C_7^{NP}} \sim [-\mathbf{0.05}, -\mathbf{0.01}]$, $\mathbf{C_9'} \sim \pm\delta$ $\mathbf{C_{10}}, \mathbf{C'_{7,10}} \sim \pm\epsilon$

- **All analysis done afterwards** using either lattice at low-recoil [Wingate et al'13] or only a fraction of all bins for Form-Factor dependent observables [Straub et al. EPJC'13] or bayesian [Bobeth et al'13] **confirmed** the impact of a **possible negative NP contribution** on the semileptonic operator O_9.

Small Controversy concerning C_9': Two claims in literature:

Our: With present data if you take **all bin data** C_9' can be positive, negative or zero but **small**.

A&S: An analysis using only [1-6] bin and low-recoil requires $C_9' \sim -C_9^{NP}$ to be **positive and large**.

Why the two analysis get different results for C_9'?

Point 1 **Large-recoil**: The single bin [1-6] is very **insensitive** to the sign of C_9'. On the contrary the 3 low-q^2 bins are quite sensitive to C_9', in particular, the 3rd shows a **strong preference** for C_9' **negative**.

Point 2 **Low-recoil**: These bins alone prefers C_9' positive (we also founded it) so any analysis focusing on low-recoil should find a preference for C_9' **positive**.

In conclusion *we reaffirm that with present data a complete full bin analysis should find no clear-cut evidence for a* **large** *positive C_9' otherwise you would be in conflict with the anomaly*. On the contrary if only low-recoil and [1-6] bins is used a C_9' positive and large is found.

Conclusions

- The analysis of LHCb data on the 4-body angular distribution of $B \to K^*(\to K\pi)\mu^+\mu^-$ using clean $P_i^{(\prime)}$, A_{FB} + radiative observables gives **the pattern**:

$$\mathbf{C_9^{NP}} \sim [-\mathbf{1.6}, -\mathbf{0.9}], \quad \mathbf{C_7^{NP}} \sim [-\mathbf{0.05}, -\mathbf{0.01}], \quad \mathbf{C_9'} \sim \pm\delta \quad \mathbf{C_{10}}, \mathbf{C'_{7,10}} \sim \pm\epsilon$$

where δ is small (at maximum half $|\mathbf{C_9^{NP}}|$) and ϵ is smaller.

- We have addressed, using symmetries, the question: is the anomaly isolated?
  - The anomaly in P_5' should also appear in P_2 in a specific way: The intriguing result is that the deviation in P_2 goes in the direction predicted by the anomaly.
  - The higher position of the zero of A_{FB} the smaller the value of P_5' at this point (for a P_4' SM-like)
  - A strong upper and lower bound on P_1: $P_5'^2 - 1 \leq P_1 \leq 1 - P_4'^2$
  - The first low-recoil bin of P_4' exhibits a 3.7σ tension between the measured and obtained value using "+" solution, pointing possibly to a statistical fluctuation or a low-recoil problem.

- All analysis done a posteriori to our analysis confirms a negative contribution to C_9. Concerning C_9', with present data a complete full bin analysis finds **no clear-cut evidence for a large positive** C_9' that would be in conflict with the anomaly.

BACK-UP slides

Computation of Primary Observables

Large-recoil: NLO QCDfactorization + $\mathcal{O}(\Lambda/m_b)$. Soft form factors $\xi_{\perp,\parallel}(q^2)$ from

$$\xi_\perp(q^2) = m_B/(m_B + m_{K^*})\mathbf{V(q^2)} \quad \xi_\parallel(q^2) = (m_B + m_{K^*})/(2E)\mathbf{A_1(q^2)} - (m_B - m_{K^*})/(m_B)\mathbf{A_2(q^2)}$$

- FF at $q^2 = 0$ and slope parameters are computed by [Khodjamirian et al.'10] (**KMPW**) using LCSR. ($\xi_\perp(0) = 0.31^{+0.20}_{-0.10}$ and $\xi_\parallel(0) = 0.10^{+0.03}_{-0.02}$). **Notice that power corrections are included here via full FF.**

Tensor form factors $\mathcal{T}_{\perp,\parallel}$ are computed in QCDF following [Beneke, Feldmann, Seidel'01,'05] including factorizable and non-factorizable contributions.

Low-recoil: LCSR are valid up to $q^2 \leq 14$ GeV^2. We extend FF determination [Bobeth & Hiller & Dyk'10] till 19 Gev^2 and cross check the consistency with **lattice** QCD.
In HQET one expects the ratios to be near one

$$\mathbf{R_1} = \frac{\mathbf{T_1(q^2)}}{\mathbf{V(q^2)}}\,, \qquad \mathbf{R_2} = \frac{\mathbf{T_2(q^2)}}{\mathbf{A_1(q^2)}}\,, \qquad \mathbf{R_3} = \frac{q^2}{m_B^2}\frac{\mathbf{T_3(q^2)}}{\mathbf{A_2(q^2)}}\,.$$

Our approach at low-recoil: we determine $T_{1,2}$ by exploiting the ratios $R_{1,2}$ allowing for up to a 20% breaking, i.e., $R_{1,2} = 1 + \delta_{1,2}$. All other form factors extrapolated from KMPW. We find perfect agreement between our determination of $T_{1,2}$ using $R_{1,2}$ and lattice data.

Integrated observables

Contact theory and experiment:

Indeed the observables are measured in bins.

Present bins: [0.1,2], [2,4.3], [4.3,8.68], [1,6], [14.18,16], [16,19] GeV^2.

The integrated version of observables $P_{1,2,3}$, $P'_{4,5,6}$ are defined by

$$\langle P_1 \rangle_{\rm bin} = \frac{1}{2\mathcal{N}_{bin}} \int_{\rm bin} dq^2 [J_3 + \bar{J}_3] \ , \quad \langle P_3 \rangle_{\rm bin} = -\frac{1}{4\mathcal{N}_{bin}} \int_{\rm bin} dq^2 [J_9 + \bar{J}_9] \quad \langle P'_5 \rangle_{\rm bin} = \frac{1}{2\mathcal{N}'_{bin}} \int_{\rm bin} dq^2 [J_5 + \bar{J}_5] \ ,$$

$$\langle P_2 \rangle_{\rm bin} = \frac{1}{8\mathcal{N}_{bin}} \int_{\rm bin} dq^2 [J_{6s} + \bar{J}_{6s}] \quad \langle P'_4 \rangle_{\rm bin} = \frac{1}{\mathcal{N}'_{bin}} \int_{\rm bin} dq^2 [J_4 + \bar{J}_4] \ , \quad \langle P'_6 \rangle_{\rm bin} = \frac{-1}{2\mathcal{N}'_{bin}} \int_{\rm bin} dq^2 [J_7 + \bar{J}_7] \ ,$$

where the normalization $\mathcal{N}'_{bin}$ is defined as

$$\mathcal{N}_{bin} = \int_{\rm bin} dq^2 [J_{2s} + \bar{J}_{2s}] \qquad \mathcal{N}'_{bin} = \sqrt{-\int_{bin} dq^2 [J_{2s} + \bar{J}_{2s}] \int_{\rm bin} dq^2 [J_{2c} + \bar{J}_{2c}]} \ .$$

The double-folded distributions give access to these observables. Similar definitions for $\langle P_i^{CP} \rangle_{\rm bin}$ with $J_i - \bar{J}_i$.

There is also a **redundant** clean observable $P'_8 = Q'$ (if there are no scalars) associated to J_8 that can be introduced for practical reasons:

$$\langle P'_8 = Q' \rangle_{\rm bin} = \frac{-1}{\mathcal{N}'_{bin}} \int_{\rm bin} dq^2 [J_8 + \bar{J}_8]$$

The concept of clean observables: origin and benefits

For a long time huge efforts were devoted (still now) to measure the position of the zero of the forward-backward asymmetry A_{FB} of $B \to K^* \mu^+ \mu^-$.

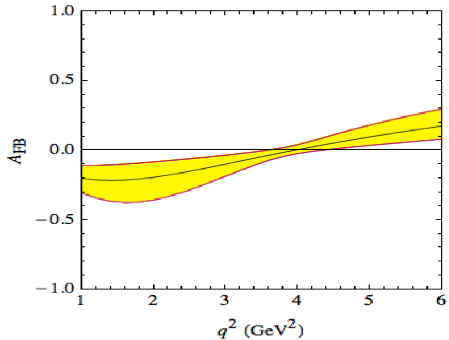

Reason:

- At LO the soft form factor dependence cancels exactly at q_0^2 (dependence appears at NLO).
- A relation among $\mathbf{C_9^{eff}}$ and $\mathbf{C_7^{eff}}$ arises at the zero:

$$\mathbf{C_9^{eff}}(q_0^2) + 2\frac{m_b M_B}{q_0^2}\mathbf{C_7^{eff}} = 0$$

The concept of clean observables: origin and benefits

The idea of **exact cancellation of the poorly known soft form factors at LO** at the zero of A_{FB} was incorporated in the construction of the transverse asymmetry (this is the meaning of the word "**clean**")

[Kruger, J.M'05] [Becirevic et al.'12]

$$P_1 = A_T^{(2)}(q^2) = \frac{J_3}{2J_{2s}} = \frac{|A_\perp|^2 - |A_{||}|^2}{|A_\perp|^2 + |A_{||}|^2} \qquad P_2 = \frac{A_T^{re}}{2} = \frac{J_{6s}}{8J_{2s}} = \frac{\mathrm{Re}(A_\perp^{L*}A_{||}^{L} - A_\perp^{R}A_{II}^{R*})}{|A_\perp|^2 + |A_{||}|^2}$$

where $A_{\perp,||}$ correspond to two transversity amplitudes of the K^*.

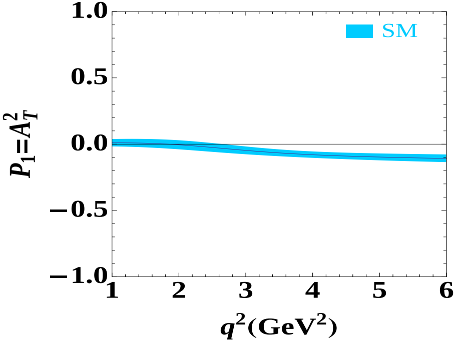

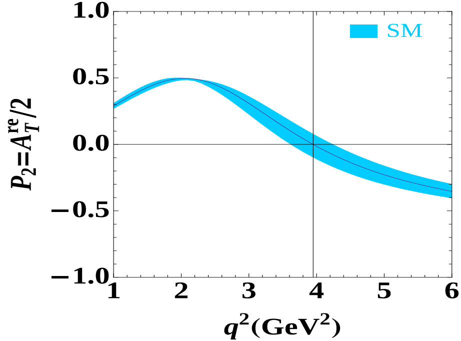

- Both asymmetries exhibit an exact cancellation of soft form factors **not only at a point** (like A_{FB}) **but in the full low-q^2 range**. First examples of **clean** observables that could be measured.
- $A_T^{(2)}$ is constructed to detect presence of RH currents ($A_\perp \sim -A_{||}$ in the SM), A_T^{re} complements A_{FB} since it contains similar information, but in a theoretically better controlled way.